

Manuscript Details

Manuscript number	EJPB_2017_669
Title	Brain targeting of resveratrol by nasal administration of chitosan-coated lipid microparticles
Article type	Research Paper

Abstract

Lipid microparticles (LMs) uncoated or coated with chitosan and containing the neuroprotective polyphenol, resveratrol were developed for its targeting to the brain via nasal administration. The lipid microparticles loaded with resveratrol (LMs-Res) were produced by melt emulsification, using stearic acid as lipid material and phosphatidylcholine as the surfactant. The chitosan coated particles LMs-Res-Ch (1.75% w/v chitosan solution) and LMs-Res-Ch-plus (8.75 % w/v chitosan solution) were prepared by adding a chitosan solution to the formed particles. The mean diameter of the particles were 68.5 ± 3.1 μm , 76.3 ± 5.2 μm and 84.5 ± 8.1 μm for LM-Res, LM-Res-Ch and LM-Res-Ch-plus respectively, suitable for nasal delivery. Chitosan coating changed the particle surface charge from a negative zeta potential value (-12.7 ± 2.1 mV) for the uncoated particles to a higher positive values respectively 24.0 ± 4.7 and 44.6 ± 3.1 mV for the chitosan coated LM-Res-Ch and LM-Res-Ch-plus. Permeation studies across human NCM460 cell monolayers demonstrated that their transepithelial electrical resistance (TEER) values were not modified in the presence of free resveratrol, unloaded LMs, loaded LMs-Res or LMs-Res-Ch. On the other hand, the TEER values decreased from 150 ± 7 to 41 ± 3 $\Omega \cdot \text{cm}^2$ in the presence of LMs-Res-Ch-plus, which corresponded to a significant increase in the apparent permeability (Papp) of resveratrol from $518 \pm 8 \times 10^{-4}$ cm/min to $750 \pm 98 \times 10^{-4}$ cm/min. In vivo studies demonstrated that no resveratrol was detected in the rat cerebrospinal fluid (CSF) after an intravenous infusion of the polyphenol. Conversely the nasal delivery of resveratrol in a chitosan suspension or encapsulated in uncoated LMs-Res dispersed in water achieved the uptake of resveratrol in the CSF with Cmax after 60 min of 1.30 ± 0.30 $\mu\text{g/ml}$ and 0.79 ± 0.15 $\mu\text{g/ml}$, respectively. However, a dramatic increase in the levels of resveratrol reaching the CSF was attained by the administration of an aqueous suspension of LM-Res-Ch-plus with a Cmax after 60 min of 9.7 ± 1.9 $\mu\text{g/ml}$. This marked increase in the CSF bioavailability was achieved without any distribution in the systemic circulation, demonstrating a direct and specific nose to brain delivery.

Keywords	resveratrol; lipid microparticles; chitosan-coating; nasal formulation; in vitro permeation studies; brain uptake.
Taxonomy	Bioadhesive, Polysaccharides, Controlled Drug Release
Corresponding Author	Santo Scalia
Corresponding Author's Institution	University of Ferrara
Order of Authors	Valentina Trotta, Barbara Pavan, Luca Ferraro, Sarah Beggiato, Daniela Traini, Larissa Gomes des Reis, Santo Scalia, Alessandro Dalpiaz
Suggested reviewers	Regina Scherließ, Eliana Souto, Shakila Rizwan, William H. Frey II

Submission Files Included in this PDF

File Name [File Type]

coverletterScaliaEJPB .doc [Cover Letter]

Graphical abstractSca EJPB.tiff [Graphical Abstract]

ManusScaliaEJPB .docx [Manuscript File]

Fig1ScaEJPB.docx [Figure]

Fig2ScaEJPB.docx [Figure]

Fig3ScaEJPB.docx [Figure]

Fig4ScaEJPB.docx [Figure]

Fig5ScaEJPB.docx [Figure]

Fig6ScaEJPB.docx [Figure]

Tab1ScaEJPB.docx [Table]

To view all the submission files, including those not included in the PDF, click on the manuscript title on your EVISE Homepage, then click 'Download zip file'.

EDITORIAL OFFICE
EUROPEAN JOURNAL OF PHARMACEUTICS AND BIOPHARMACEUTICS

Dear Editor,

Please find enclosed the manuscript: **“Brain targeting of resveratrol by nasal administration of chitosan-coated lipid microparticles”** by Valentina Trotta , Barbara Pavan, Luca Ferraro, Sarah Beggiato, Daniela Traini, Larissa Gomes Des Reis, Santo Scalia and Alessandro Dalpiaz , that we would like to submit for publication in the EUROPEAN JOURNAL OF PHARMACEUTICS AND BIOPHARMACEUTICS.

The submitted manuscript comprises original research that has not been published previously and it is not under consideration for publication elsewhere. All authors have read and approved the text and consent to its publication. The authors report no conflicts of interest.

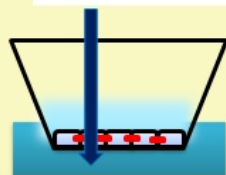
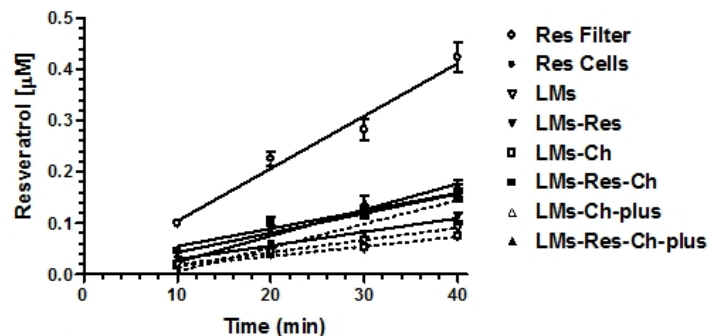
The submitted manuscript describes the development of a chitosan-coated lipid microparticle system loaded with the natural neuroprotective agent, resveratrol and designed for its direct nose-to-brain delivery. Although the activity of resveratrol against neurological disorders such as Alzheimer’s and Parkinson’s diseases has been reported, these pharmacological beneficial effects are compromised *in vivo* and fail to translate into clinical applications, because of resveratrol poor stability, high metabolism and limited bioavailability in the CNS. In order to overcome this problem, the nasal administration of resveratrol incorporated in nanoemulsion and nanosuspension has been previously reported. A new approach is described in the submitted study, based on the nasal delivery of lipid microparticles loaded with resveratrol and coated with chitosan. The developed carrier exhibits several advantages compared to the published systems, including higher biocompatibility, a greater enhancement of resveratrol bioavailability in the rat brain (12 fold increase vs 6-7 fold reported in the previous studies) and especially a very specific delivery of resveratrol in the CNS with no distribution in the systemic circulation (in the previous studies 24-35% of the nasal administered resveratrol was found in the rat blood). To the best of our knowledge, this work represents the first example of the use of lipid microparticles as carrier for the delivery of resveratrol to the CNS via nasal administration. The results reported in the submitted manuscript indicate that the nasal administration of chitosan-coated lipid microparticles represents a promising system to enhance the effect of resveratrol in the treatment of brain disorders.

Yours sincerely

Dr. Santo Scalia

Dipartimento di Scienze Chimiche e Farmaceutiche
via Fossato di Mortara, 17-19
44100 Ferrara – Italy ; Phone: +39-0532-455919; E-mail: sls@unife.it

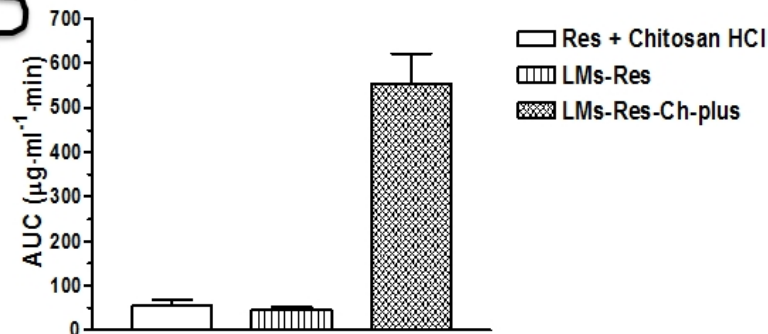
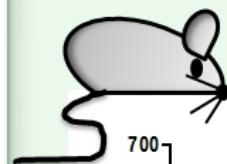
1. Resveratrol (Res) in vitro cell permeability using LMs formulations coated and uncoated with chitosan (Ch)



	P_{app} ($\times 10^{-4}$ cm/min)
LMs-Res	390 ± 20
LMs-Res-Ch	510 ± 80
LMs-Res-Ch-plus	750 ± 98



2. Res in cerebrospinal fluid after in vivo nasal administration of LMs formulations coated and uncoated with chitosan



1
2
3 **Brain targeting of resveratrol by nasal administration of chitosan-coated lipid**
4 **microparticles**
5
6
7

8
9 Valentina Trotta ^a, Barbara Pavan^b, Luca Ferraro^b, Sarah Beggiato^b, Daniela Traini^c, Larissa Gomes
10 Des Reis^c, Santo Scalia^{a,*} and Alessandro Dalpiaz ^a
11
12

13
14
15
16 ^a Department of Chemical and Pharmaceutical Sciences, University of Ferrara, Ferrara, Italy
17

18 ^b Department of Life Sciences and Biotechnology, University of Ferrara, Ferrara, Italy
19

20
21 ^c Discipline of Pharmacology, School of Medicine, University of Sydney and Woolcock Institute of
22 Medicinal Research, Sydney, Australia
23
24
25
26
27
28
29
30
31
32
33
34
35

36 * Corresponding author :
37

38 Dr. Santo Scalia

39 Dipartimento di Scienze Chimiche e Farmaceutiche

40 Via Fossato di Mortara, 17

41 44121 Ferrara

42 e-mail: sls@unife.it

43 tel: +39-0532-455919
44
45
46
47
48
49
50
51
52
53
54
55
56
57
58
59

ABSTRACT

Lipid microparticles (LMs) uncoated or coated with chitosan and containing the neuroprotective polyphenol, resveratrol were developed for its targeting to the brain via nasal administration. The lipid microparticles loaded with resveratrol (LMs-Res) were produced by melt emulsification, using stearic acid as lipid material and phosphatidylcholine as the surfactant. The chitosan coated particles LMs-Res-Ch (1.75% w/v chitosan solution) and LMs-Res-Ch-plus (8.75 % w/v chitosan solution) were prepared by adding a chitosan solution to the formed particles. The mean diameter of the particles were $68.5\pm 3.1\ \mu\text{m}$, $76.3\pm 5.2\ \mu\text{m}$ and $84.5\pm 8.1\ \mu\text{m}$ for LMs-Res, LMs-Res-Ch and LMs-Res-Ch-plus respectively, suitable for nasal delivery. Chitosan coating changed the particle surface charge from a negative zeta potential value ($-12.7\pm 2.1\ \text{mV}$) for the uncoated particles to a higher positive values respectively, 24.0 ± 4.7 and $44.6\pm 3.1\ \text{mV}$ for the chitosan coated LM-Res-Ch and LM-Res-Ch-plus. Permeation studies across human NCM460 cell monolayers demonstrated that their transepithelial electrical resistance (TEER) values were not modified in the presence of free resveratrol, unloaded LMs, loaded LMs-Res or LMs-Res-Ch. On the other hand, the TEER values decreased from 150 ± 7 to $41\pm 3\ \Omega\text{-cm}^2$ in the presence of LMs-Res-Ch-plus, which corresponded to a significant increase in the apparent permeability (P_{app}) of resveratrol from $518\pm 8\times 10^{-4}\ \text{cm}/\text{min}$ to $750\pm 98\times 10^{-4}\ \text{cm}/\text{min}$. In vivo studies demonstrated that no resveratrol was detected in the rat cerebrospinal fluid (CSF) after an intravenous infusion of the polyphenol. Conversely, the nasal delivery of resveratrol in a chitosan suspension or encapsulated in uncoated LMs-Res dispersed in water achieved the uptake of resveratrol in the CSF with C_{max} after 60 min of $1.30\pm 0.30\ \mu\text{g}/\text{ml}$ and $0.79\pm 0.15\ \mu\text{g}/\text{ml}$, respectively. However, a dramatic increase in the levels of resveratrol reaching the CSF was attained by the administration of an aqueous suspension of LMs-Res-Ch-plus with a C_{max} after 60 min of $9.7\pm 1.9\ \mu\text{g}/\text{ml}$. This marked increase in the CSF bioavailability was achieved without any

119
120
121 distribution in the systemic circulation, demonstrating a direct and specific nose to brain
122
123 delivery.
124
125
126
127
128

129 Keywords : resveratrol, lipid microparticles, chitosan-coating, nasal formulation, in vitro
130
131 permeation studies, brain uptake
132
133
134
135
136
137
138
139
140
141
142
143
144
145
146
147
148
149
150
151
152
153
154
155
156
157
158
159
160
161
162
163
164
165
166
167
168
169
170
171
172
173
174
175
176
177

178
179
180 **1. Introduction**
181
182
183

184 The polyphenol resveratrol is a natural compound, that is found in different types of fruits,
185 vegetables and also in red wine [1]. This polyphenolic compound exists in two isoforms *cis*-
186 and *trans*-resveratrol, the isomer *trans* being more active than the *cis*-form [2].
187
188

189 Resveratrol has attracted the attention of researchers due to its therapeutic effects against
190 various illness, such as cardiovascular diseases [3], diabetes [4], neurodegenerative diseases
191 [5], lung inflammation [6] and cancer [7]. *In vitro* and *in vivo* investigations have pointed out
192 that the beneficial properties of resveratrol are correlate to its anti-inflammatory and anti-
193 oxidant capabilities [8-10].
194
195
196
197
198
199
200

201 Resveratrol has been reported to exert the anti-inflammatory activity through several
202 mechanisms that bring to the inhibition of both the transcription and the release of different
203 inflammatory mediators [8,9]. Furthermore, resveratrol has also been shown to protect the
204 cell from the oxidative damage by means of its anti-oxidant capability based on scavenging of
205 free radicals [10].
206
207
208
209
210
211

212 Specifically for central nervous system diseases, resveratrol has been reported to be
213 effective against neurologic disorders such as Alzheimer's and Parkinson's diseases, brain
214 ischemia and epilepsy [11-14]. Several mechanisms have been advocated for the
215 neuroprotective activity of resveratrol, including its anti-oxidant and anti-inflammatory action
216 [14-16], stabilization of neuronal mitochondrial function, improvement of cerebral blood
217 flow, protection of dopaminergic neurons, inhibition of formation and aggregation of
218 amyloid- β peptide and activation of sirtuin 1 [13-15,17-19].
219
220
221
222
223
224
225
226

227 However, these pharmacological beneficial effects are difficult to translate into clinical
228 applications because of resveratrol limited chemical stability, poor aqueous solubility (ca. 3
229 mg/100 mL) and high metabolism [2,20] which limit its *in vivo* bioavailability. To
230
231
232
233
234
235
236

237
238
239 circumvent this drawback, different strategies have been developed including the use of drug
240
241 delivery systems such as cyclodextrins, liposomes, nano- and micro-particles [2, 21-23]. In
242
243 particular, lipid microparticles (LMs) which consist of a natural lipid-based solid core
244
245 stabilized by a layer of surfactant at the outer shell, exhibit several favourable characteristics
246
247 as drug carrier including high biocompatibility and biodegradability, low production cost,
248
249 adequate physico-chemical stability, protection of the incorporated active substance against
250
251 degradation and modulation of its release [24]. Moreover, due to their micron dimensions
252
253 LMs have additional advantages compared to liposomes and lipid nanoparticles, including
254
255 simpler production and characterization methods, reduced amount of required surfactant,
256
257 higher stability and loading capacity [24,25].
258
259

260
261 An additional specific problem for the delivery of appropriate therapeutic resveratrol
262
263 concentrations in the central nervous system (CNS) is the presence of the blood brain barrier
264
265 (BBB) which is particularly difficult to permeate [13,15,26]. Indeed, even if it is known that
266
267 resveratrol is able to permeate in the brain from the blood stream in rodents [27] and humans
268
269 [28], its distribution in the central nervous system appears very poor in comparison to other
270
271 tissues [29]. Since the brain is connected to the nose via the olfactory portion of the nasal
272
273 mucosa [18,30-33], the latter region represents an alternative pathway for the direct delivery
274
275 of active substances to the central nervous system by-passing the BBB. For instance, it has
276
277 been recently reported that the nasal administration of deferoxamine or insulin can be
278
279 efficacious against Parkinson's or Alzheimer's diseases, respectively [34,35]. Moreover, the
280
281 intranasal drug administration route is non-invasive, easy to access and with favourable
282
283 patient compliance [18,30,32]. In order to enhance the efficacy of nose to brain targeting, the
284
285 problem of limited residence time due to the rapid mucociliary clearance and relatively low
286
287 nasal absorption should be addressed. With regard to this, nasal powder preparations offer the
288
289 advantage of improved residence time on the mucosal surface compare to liquid formulations.
290
291
292
293
294
295

296
297
298 Moreover, the addition of excipients such as bioadhesive carriers and penetration enhancers
299
300 should further enhance the bioavailability. Among these excipients, chitosan, a cationic
301
302 polysaccharide of natural origin, has been reported to increase nasal delivery of active drugs
303
304 due to its mucoadhesive properties [36,37] and ability to promote the reversible opening of
305
306 cellular tight junctions thereby increasing paracellular transport [36,37].
307

308
309 Aim of this work was the development and characterization of resveratrol-loaded LMs
310
311 without or with chitosan coating, as system for the delivery of the polyphenol to the CNS
312
313 through the olfactory region. The influence of the LMs on cell viability, resveratrol transport
314
315 and uptake using NCM 460 cells was evaluated. Moreover, *in vivo* studies were performed on
316
317 rats comparing the intravenous infusion of a resveratrol solution with the nasal administration
318
319 of free or microencapsulated resveratrol. The time course of resveratrol levels in blood and
320
321 cerebrospinal fluid were measured after the intravenous and intranasal administration.
322
323
324
325
326
327

328 **2. Materials and methods**

329 330 331 332 *2.1. Materials*

333
334 Resveratrol (*trans*-3,4',5-trihydroxystilbene) was from Fragon Italia (Bologna, Italy).
335
336 Tristearin, glyceryl behenate and stearic acid were supplied by Sigma Aldrich (Steinheim,
337
338 Germany), Gattefosse' (Cedex, France) and Fluka Chemie (Buchs, Switzerland), respectively.
339
340 The medium-molecular weight chitosan was obtained by Sigma Aldrich (Steinheim,
341
342 Germany). Phosphatidylcholine and Tween 80 were supplied by Cargill (Hamburg, Germany)
343
344 and Fluka Chemie (Bucks, Switzerland), respectively. Chitosan hydrochloride was purchased
345
346 from FMC Biopolymer AS (Drammen, Norway). Bond-Elut C18-, Isolute C18- and Isolute
347
348 MF C18- silica cartridges (sorbent weight, 200 mg) were from Agilent Technologies
349
350
351
352
353
354

355
356
357 (Waldbronn, Germany) and International Sorbent Technology (Hegoed, UK), respectively.
358

359 The high-performance liquid chromatographic (HPLC)-grade methanol, acetonitrile and water
360 were obtained from Sigma–Aldrich (Steinheim, Germany).
361

362
363 NCM-460 cells were kindly provided by Dr. Antonio Strillacci, University of Bologna, Italy.
364

365 The male Sprague–Dawley rats were provided by Charles-River (Milan, Italy).
366
367

368 369 370 *2.2. High-performance liquid chromatography* 371

372 High performance liquid chromatography (HPLC) was used in order to quantify
373 resveratrol. The HPLC system was equipped with a Model LabFlow 3000 pump (LabService
374 Analytica, Bologna, Italy), a Model 7125 injection valve with a 10 μ L sample loop
375
376 (Rheodyne, Cotati, CA, USA) and a Model 975-UV variable wavelength UV–vis detector
377
378 (Jasco, Tokyo, Japan) set at 306 nm. Separations were achieved on a 5- μ m Zorbax SB C-18
379
380 column (150 x 4.6 mm i.d.; Agilent Technologies) fitted with a guard column (5- μ m particles,
381
382 4 mm \times 2 mm i.d.; Phenomenex, Torrance, CA, USA) and eluted with 65% (v/v) methanol in
383
384 water containing 0.4% (v/v) acetic acid. Chromatography was performed at ambient
385
386 temperature at a flow rate of 0.8 mL/min. For the *in vivo* studies, resveratrol analysis in
387
388 biological fluid was carried out with a mobile phase composed of 40% (v/v) acetonitrile in
389
390 water containing 0.4% (v/v) acetic acid and 0.75 mM EDTA, to achieve satisfactory
391
392 resolution between resveratrol and the internal standard (quercetin) peaks. The flow-rate was
393
394 0.8 mL/min and the eluent was monitored at 306 nm for resveratrol and at 370 nm for
395
396 quercetin. Data acquisition and processing were performed with a personal computer using
397
398 Clarity Lite chromatographic software (DataApex, Prague, Czech Republic). The identities of
399
400 resveratrol and quercetin (internal standard) peaks were assigned by co-chromatography with
401
402 the authentic standards.
403
404
405
406
407
408
409
410
411
412
413

414
415
416 The quantification of resveratrol was carried out by the peak area correlated with the
417
418 predetermined standard curve over the range 0.25-100 µg/mL. The calibration curve was
419
420 linear (n=8, R =0.994, P < 0.001). The chromatographic precision, represented by relative
421
422 standard deviations (RSD), was evaluated by repeated analysis (n = 6) of the same sample
423
424 solution containing resveratrol at a concentration of 10 µg/mL. The RSD value was 1.3%.
425

426
427 For CSF simulation, standard aliquots of balanced solution (PBS Dulbecco's without
428
429 calcium and magnesium) in the presence of 0.45 mg/mL BSA were employed [38,39]. For the
430
431 assay of resveratrol in CSF, the chromatographic precision was evaluated by repeated analysis
432
433 (n = 6) of the same sample solution containing 5 µg/mL resveratrol (RSD = 4.0 %) in
434
435 simulated CSF and calibration curves of peak areas versus concentration were generated in
436
437 the range 0.1-15 µg/mL (n =6, R =1, P < 0.001).
438

439
440 Resveratrol quantification in rat blood was on the basis of peak area for the ratio
441
442 resveratrol/quercetin (internal standard). Calibration standards were prepared by spiking
443
444 blood extracts with the internal standard (quercetin) and with known amounts of resveratrol
445
446 corresponding to blood concentrations in the range 0.25-20 µg/mL. These solutions were
447
448 analysed by HPLC and the obtained calibration curves of peak area ratios versus
449
450 concentrations were linear (n=6, R=0.993, P<0.001). The precision of the method, evaluated
451
452 by replicate analyses (n= 6) of rat blood extract containing the internal standard (quercetin),
453
454 and resveratrol at a level of 10 µg/mL, was demonstrated by relative standard deviations < 2.0
455
456 %.
457
458

459 460 461 *2.3. Lipid microparticle preparation*

462
463 LMs loaded with resveratrol were prepared using the melt oil/water emulsification
464
465 technique, via a phase inversion procedure (aqueous phase poured into the molten lipid) in
466
467
468
469
470
471
472

473
474
475 order to avoid loss of both, resveratrol and excipient during the particles preparation
476
477 procedure.

478
479 In brief, the hot aqueous phase (40 mL) in which the surfactant phosphatidylcholine
480 (1.75% w/v) was dispersed, was poured into the melted lipid phase (3.8 g) in which
481 resveratrol (0.35 g) was dispersed. The two phases were mixed using an Ultra Turrax T-25
482 mixer (IKA-Werk, Staufen, Germany) at 13500 rpm for 1.30 min at a temperature of 75-85
483 °C. The obtained emulsion was cooled to room temperature using an ice bath under magnetic
484 stirring and then subject to centrifugation at 6000 rpm for 15 min. Finally, the precipitate was
485 lyophilized in order to obtained water-free microparticles.
486
487

488
489 The LMs coated with chitosan were prepared by adding, under stirring, a chitosan solution
490 (1.75 %, w/v) in aqueous acetic acid (pH 4.2) to the LMs suspension formed during the
491 cooling phase of the emulsion. Throughout the manuscript the LMs loaded with resveratrol, in
492 the absence and in presence of chitosan (Ch) are indicated as LMs-Res and LMs-Res-Ch,
493 respectively. Moreover, a LM formulation loaded with resveratrol and coated with chitosan,
494 using a higher concentration of the polysaccharide in aqueous acetic acid (8.75%, w/v), was
495 also prepared and indicated as LMs-Res-Ch-plus.
496
497

498
499 Unloaded LMs were also prepared with the same procedures, but omitting resveratrol.
500
501

502 503 504 505 506 507 508 509 510 511 512 513 *2.4. Particle morphology*

514
515 The LM morphology was observed using a bench top scanning electron microscopy (SEM)
516 (JEOL JMC-6000 SEM, Tokyo, Japan) at 15 kV. Powders of LMs formulations were
517 randomly placed on the top of carbon sticky tapes that was previously attached on the
518 aluminum stubs. Then the samples were coated with gold for two minutes by the Smart coater
519 (JOEL, Tokyo, Japan).
520
521
522
523
524
525
526
527
528
529
530
531

532
533
534 *2.5. Particles size analysis*
535

536 Laser diffraction (Mastersizer 3000, HYDRO; Malvern, Worcestershire, United
537 Kingdom) was used in order to measure the particle size distribution of LM formulations. The
538 LMs were dispersed in water with 0.25% Tween 80 to obtain a c.a. 0.22 mg/mL particle
539 concentration for each sample and analyzed with a feed pressure of 4 bar, obscuration interval
540 between 0.1 to 15% and a refractive index of 1.762. Analyses were performed in triplicate.
541 Particle surface charge was evaluated by dynamic laser light scattering using a folded
542 capillary zeta cell on a Malvern Nano Series ZS Instrument at 25°C. Light scattering data
543 were obtained at a detection angle of 173°. Particles were dispersed in filtered (0.2 µm)
544 deionized water. Six measurements were performed for each sample.
545
546
547
548
549
550
551
552
553
554
555

556
557 *2.6. Resveratrol loading*
558

559 The LMs (10 mg) were dispersed in ethanol (4 mL) in sealed glass vials, heated (80 °C, 5
560 min) and sonicated for 10 min. The obtained samples were diluted to volume (20 mL) with
561 methanol and filtered using 0.45 µm membrane filters and assayed by HPLC. The polyphenol
562 loading was determined as the percentage ratio between the amount of resveratrol assayed in
563 the LMs and the total weight of the particle sample.
564
565
566
567
568
569

570 The encapsulation efficiency was calculated as the percentage ratio between the quantity of
571 resveratrol entrapped in the microparticles and the amount of polyphenol added to the melted
572 lipid phase during preparation. The results were the average of three determinations.
573
574
575
576
577

578
579 *2.7. In vitro resveratrol release*
580

581 Resveratrol dissolution and release from the LMs were evaluated by adding raw resveratrol
582 (ca 0.8 mg) or LMs, containing an equivalent amount of the polyphenol, to 80 mL of
583 phosphate buffer (0.05 M, pH 7.4). The samples were kept under mechanical stirring at 50
584
585
586
587
588
589
590

591 rpm and 37 °C. At predetermined time intervals, 1 mL aliquots of the medium were
592
593
594 withdrawn and replaced with an equal volume of fresh fluid. The test samples were filtered
595
596 (0.45 µm) and assayed by HPLC. The resveratrol release (%) was calculated from the total
597
598 polyphenol content of the LM preparations, which was calculated by extraction of the
599
600 particles after the release experiment, using the procedure outlined in the previous Section.
601
602
603 Data were determined from the average of at least six experiments.
604
605
606
607

608 *2.8. NCM460 cell culture condition*

609

610 The NCM460 cell line was grown in DMEM + Glutamax supplemented with 10% fetal
611
612 bovine serum (FBS), 100 U/mL penicillin, and 100 µg/mL streptomycin at 37 °C in a
613
614 humidified atmosphere of 95%, with 5% of CO₂. For maximum viability, NCM460 cells were
615
616 subcultured in fresh and spent growth medium in 1:1 ratio. All cell culture reagents were
617
618 provided by Invitrogen (Life Technologies, Milan, Italy).
619
620
621
622
623

624 *2.9. Differentiation of NCM460 cells to polarized monolayers*

625

626 Differentiation to NCM460 cell monolayers was performed essentially according to the
627
628 method reported by Ferretti and co-workers [40]. Briefly, after two passages, confluent
629
630 NCM460 cells were seeded at a density of 105 cells/mL in a 1:1 ratio of fresh and spent
631
632 culture medium in 12-well Millicell inserts (Millipore, Milan, Italy) consisting of 1.0 µm pore
633
634 size polyethylene terephthalate (PET) filter membranes, whose surface was 1.12 cm². Filters
635
636 were presoaked for 24 h with fresh culture medium, and then the upper compartment (apical,
637
638 A) received 400 µL of the diluted cells, whereas the lower (basolateral, B) received 2 mL of
639
640 the medium in the absence of cells. Half volume of the culture medium was replaced every 2
641
642 days with fresh medium to each of the apical and basolateral compartments. The integrity of
643
644 the cell monolayers was monitored by measuring the transepithelial electrical resistance
645
646
647
648
649

650
651
652 (TEER) by means of a voltmeter (Millicell-ERS; Millipore, Milan, Italy). The measured
653
654 resistance value was multiplied by the area of the filter to obtain an absolute value of TEER,
655
656 expressed as $\Omega \cdot \text{cm}^2$. The background resistance of blank inserts not plated with cells was
657
658 around $35 \Omega \cdot \text{cm}^2$ and was deducted from each value. The homogeneity and integrity of the
659
660 cell monolayer were also monitored by phase contrast microscopy. Based on these
661
662 parameters, cell monolayers reached confluence and epithelial polarization after 6 days, and
663
664 monolayers with a TEER stable value around $160 \Omega \cdot \text{cm}^2$ were used for permeation studies. At
665
666 this point, the medium was replaced with low serum fresh medium (1% FBS) in both the
667
668 apical and basal compartments.
669
670
671
672

673 *2.10. Permeation studies across cell monolayers*

674
675 For permeation studies, inserts were washed twice with pre-warmed PBS buffer in the
676
677 apical (A, 400 μL) and basolateral (B, 2 mL) compartments, and then PBS buffer containing 5
678
679 mM glucose at 37 °C was added to the apical compartment. The apical compartments
680
681 received the following formulations containing an equivalent amount of resveratrol (0.114
682
683 mg/mL): raw resveratrol, LMs-Res, LMs -Res-Ch and LMs-Res-Ch-plus, raw resveratrol with
684
685 the unloaded microparticles LMs, LMs-Ch and LMs-Ch-plus. During permeation
686
687 experiments, Millicell inserts loaded with the powder preparations were continuously swirled
688
689 on an orbital shaker (100 rpm; model 711/CT; ASAL, Cernusco, Milan, Italy) at 37 °C. At
690
691 programmed time points, the inserts were removed and transferred into the subsequent wells
692
693 containing fresh PBS, and then basolateral PBS was harvested, filtered through regenerated
694
695 cellulose filters (0.45 μm), and injected (10 μL) into the HPLC system for the determination
696
697 of the concentration of resveratrol. At the end of incubation the apical slurries were
698
699 withdrawn, filtered, and injected into the HPLC system (10 μL). After the withdrawal of
700
701 apical samples, 400 μL of PBS was inserted in the apical compartments and TEER
702
703
704
705
706
707
708

709
710
711 measurements were performed. Permeation experiments of free resveratrol were also
712
713 conducted using cell-free inserts in the same conditions described above. All the values
714
715 obtained were the mean of three independent experiments. Apparent permeability coefficients
716
717 (P_{app}) of resveratrol were calculated according to the following equation [41-43] :

$$P_{app} = \frac{\frac{dc}{dt} V_r}{S_A C} \quad (1)$$

720
721
722
723
724
725
726
727
728
729
730 where P_{app} is the apparent permeability coefficient in cm/min; dc/dt is the flux of drug across
731
732 the filters, calculated as the linearly regressed slope through linear data; V_r is the volume in
733
734 the receiving compartment (basolateral = 2 mL); S_A is the diffusion area (1.13 cm²); and C is
735
736 the compound concentration in the donor chamber (apical) detected at 60 min and chosen as
737
738 approximate apical concentration.

739 740 741 742 743 744 *2.11. In vivo resveratrol administration and quantification*

745
746 Male Wistar rats (200–250 g) anesthetized during the experimental period received a
747
748 femoral intravenous infusion of 0.2 mg/mL resveratrol dissolved in a medium constituted by
749
750 20% (v/v) DMSO and 80% (v/v) physiologic saline, with a rate of 0.2 mL/min for 5 min. At
751
752 the end of infusion and at fixed time points, blood samples (100 μ L) were collected and CSF
753
754 samples (50 μ L) were withdrawn by cisternal puncture method described by van den Berg et
755
756 al. [44], as previously reported [45]. Briefly, before the experiments the rats were anesthetized
757
758 and fixed in a stereotaxic apparatus, after shaving of the skin overlying the neck. A needle
759
760 connected to a syringe by means of polyethylene tubing and filled with sterile filtered water
761
762 was attached to a holder of the stereotaxic frame. Following the appropriate stereotaxic
763
764
765
766
767

768
769
770 coordinates [44], the needle was brought into position to carry out the puncture. Before
771
772 puncturing, an air bubble was drawn into the needle with the syringe at the other end of the
773
774 collection tubing. For puncturing, the needle was gently moved through the skin and muscles
775
776 toward the cisterna magna. During the needle placement, the syringe plunger was pulled back
777
778 to create negative pressure; thereafter, the needle advancement was continued until the air
779
780 bubble moved into the tubing followed by CSF. Then, the syringe and the tubing were
781
782 disconnected from the CSF collection system and a Hamilton syringe was attached to the CSF
783
784 collection tubing and used for CSF withdrawal. After sampling, the Hamilton syringe was
785
786 disconnected and the tubing was closed with a clamp. Subsequent samples were taken by
787
788 removing the clamp from the tubing, followed by attachment of the Hamilton syringe. This
789
790 procedure requires a single needle stick and allows the collection of serial (40–50 μL) CSF
791
792 samples which are virtually blood-free. A total volume of about 150 μL of CSF was collected
793
794 during the experimental session. Considering that the total CSF volume in adult rats ranges
795
796 from 300 to 400 μL [46,47], 50 μL of CSF should represent about 12% of the original total
797
798 volume.
799
800

801
802 Four rats were employed for femoral intravenous infusions. The CSF samples (10 μL)
803
804 were immediately injected into HPLC system for resveratrol assay. The rat blood samples
805
806 were subjected to solid-phase extraction using a Isolute MF C18-silica cartridge. To a portion
807
808 (0.1 mL) of the rat blood, 0.1 mL of the standard solution (100 μM quercetin in water
809
810 containing 1% DMSO) were added. After mixing, the sample was applied by positive
811
812 pressure (flow-rate, ca. 1 mL/min) to a pre-conditioned (2 mL of methanol and then 2 mL of
813
814 water containing 0.75 mM EDTA) Isolute MFC18 cartridge which was washed successively
815
816 with 4 mL of water containing 0.75 mM EDTA and 2 mL of 15% methanol in water. After
817
818 light drying by vacuum, the cartridge was eluted with 2 mL of methanol. The latter fraction
819
820 was reduced to dryness under a nitrogen stream, the residue reconstituted in 150 μL of mobile
821
822
823
824
825
826

827
828
829 phase, subjected to centrifugation (15000 g for 5 min) and a portion (10 μ L) of the obtained
830
831 supernatant injected onto the HPLC column.
832

833
834 For the determination of resveratrol recovery from the blood matrix, rat blood (0.1 mL)
835
836 was spiked with 0.1 mL of the internal standard solution (100 μ M quercetin) and with
837
838 resveratrol (1 and 10 μ g/mL). The samples were processed by solid-phase extraction as
839
840 outlined above and the recovery was calculated as the percent ratio of the peak areas of
841
842 resveratrol extracted from the test samples with that obtained by direct injection of an
843
844 equivalent amount of the analyte dissolved in the mobile phase. The recovery of resveratrol
845
846 from rat blood was \geq 80.3%.
847
848
849

850 The *in vivo* half-life of resveratrol in the blood was calculated by nonlinear regression
851
852 (exponential decay) of terminal concentration values in the time range between 1h and 6h
853
854 after infusion and confirmed by linear regression of the log concentration values versus time.
855
856 Nasal administration of resveratrol was performed on anesthetized rats laid on their backs. An
857
858 aliquot (50 μ L) of an aqueous suspension of resveratrol (2 mg/mL) was introduced in each
859
860 nostril of the rats using a semiautomatic pipet which was attached to a short polyethylene
861
862 tubing. The aqueous suspension of resveratrol was obtained in the absence and in the presence
863
864 of chitosan hydrochloride (7.5 mg/mL), as absorption enhancer. The tubing was inserted
865
866 approximately 0.6–0.7 cm into each nostril. After the administration, blood (100 μ L) and CSF
867
868 samples (50 μ L) were collected at fixed time points and analysed as described above. Four
869
870 rats were employed for nasal administration of each type of resveratrol suspension. The
871
872 resveratrol loaded microparticles uncoated (LMs-Res, 37 mg/mL) and coated with chitosan
873
874 (LMs-Res-Ch-plus, 30.3 mg/mL) were introduced in each rat nostril as a 50 μ L aqueous
875
876 suspension. After administration of the formulations, blood (100 μ L) and CSF samples (50
877
878 μ L) were collected at fixed time points, and analysed as described above. Four rats were
879
880 employed for nasal administration of the suspension of each type of microparticles. All *in*
881
882
883
884
885

886
887
888 *in vivo* experiments were performed in accordance with the European Communities Council
889
890 Directive of September 2010 (2010/63/EU), the Declaration of Helsinki, and the Guide for the
891
892 Care and Use of Laboratory Animals as adopted and promulgated by the National Institutes of
893
894 Health (Bethesda, Maryland). The protocol of all the *in vivo* experiments has been approved
895
896 by the Local Ethics Committee (University of Ferrara, Ferrara, Italy). Every effort was
897
898 completed to reduce the number of animals and their suffering. The area under concentration
899
900 curves of resveratrol in the CSF (AUC, $\mu\text{g mL}^{-1} \text{ min}$) were calculated by the trapezoidal
901
902 method.
903
904
905
906

907 *2.12. Statistical analysis*

909
910 Statistical analysis of data were performed by one way ANOVA followed by Bonferroni
911
912 post-test. $P < 0.05$ was considered statistically significant. All the calculations were
913
914 performed by using the computer program Graph Pad Prism (GraphPad Software
915
916 Incorporated, La Jolla, CA, USA), which was employed also for the linear regression of the
917
918 cumulative amounts of the compounds in the basolateral compartments of the Millicell
919
920 systems. The quality of fit was determined by evaluating the correlation coefficients (R) and P
921
922 values.
923
924
925
926
927

928 **3. Results and discussion**

929 930 931 932 *3.1. Lipid microparticle preparation and characterization*

935
936 In order to produce an inhalable resveratrol powder formulation for nasal delivery, LM
937
938 based systems were used as the polyphenol carrier. For this study, a melt emulsification
939
940 technique was employed to manufacture the LMs loaded with resveratrol since it avoids the
941
942
943
944

945 use of organic solvents. Moreover, this technique has been previously utilized to prepare LMs
946
947 for in vitro nasal deposition studies [23].
948
949

951 Various lipids (tristearin, glyceryl behenate and stearic acid) in combination with
952 phosphatidylcholine as biocompatible surfactant were evaluated for the preparation of the
953 LMs. The polyphenol loading into the lipid microparticles was $6.8 \pm 0.1 \%$, $5.5 \pm 0.4\%$ and
954 $6.6 \pm 0.8 \%$ (w/w) corresponding to an entrapment efficiency of $80.6 \pm 1.4 \%$, $65.9 \pm 4.2 \%$
955 and $78.6 \pm 8.1 \%$ for LMs manufactured with tristearin, glyceryl behenate and stearic acid,
956 respectively. These data indicated that the type of lipid used influences the microparticle
957 entrapment capacity. This phenomenon is probably due to different affinity between the
958 polyphenol and the examined lipids [25].
959
960
961
962
963
964
965
966
967

968 The release of resveratrol from the LMs was significantly lower (ANOVA) than its
969 dissolution, thus suggesting the entrapment of resveratrol in the lipid particle matrix (Figure
970 1). Differences among the LMs based on the various lipids were statistically significant at 60
971 min (stearic acid-LMs versus tristearin-LMs) and 120 min (stearic acid-LMs versus
972 tristearin-LMs and glyceryl behenate-LMs versus tristearin-LMs). The microparticles
973 prepared with stearic acid (LMs-Res) achieving the highest release rate (Figure 1) were
974 selected for further experimentation, in order to enhance the amount of resveratrol available
975 to the nasal mucosa.
976
977
978
979
980
981
982
983
984

985 A key factor which limits the effectiveness of products for nasal administration is their
986 rapid removal by mucociliary clearance. In order to prolong the residence time of powder
987 formulations on the nasal mucosal, the addition of excipients with mucoadhesive properties
988 has elicited a considerable interest [36]. Among the commonly used bioadhesive excipients
989 for nasal powder formulations, chitosan exhibits several advantages including
990 biocompatibility and absorption enhancing properties [36,37,48]. Accordingly, LM
991 formulations based on stearic acid and coated with chitosan were manufactured. The coating
992
993
994
995
996
997
998
999
1000
1001
1002
1003

1004
1005
1006 was achieved by mixing chitosan solutions at different concentrations (1.75 % or 8.75 %,
1007
1008 w/v) with the LM suspension [22] and the obtained preparations were indicated as LMs-Res-
1009
1010 Ch (1.75% chitosan solution) and LMs-Res-Ch-plus (8.75% chitosan solution). The
1011
1012 resveratrol content of the latter particle formulations was $6.4 \pm 0.5\%$ and $6.8 \pm 0.6\%$ (w/w),
1013
1014 that corresponded to an entrapment efficiency of 76.5% and 81.0%, for LMs-Res-Ch and
1015
1016 LMs-Res-Ch-plus, respectively. These results indicated that coating of the particles with
1017
1018 chitosan did not significantly affect the polyphenol loading of the LMs, in comparison with
1019
1020 the uncoated lipid particles.
1021

1022
1023 Release studies performed on the microparticles coated with chitosan indicated that, with
1024
1025 the exception of the values at 15 min, there was not significant difference (ANOVA)
1026
1027 compared to the curve measured for the uncoated LM-Res (profiles not shown). SEM analysis
1028
1029 of the stearic acid-based LM-Res, LM-Res-Ch and LM-Res-Ch-plus revealed an irregular
1030
1031 shape with a rough surface due to the presence of fragments which increased for the LM-Res-
1032
1033 Ch and LM-Res-Ch-plus systems (Figure 2). The SEM micrographs indicated for all LM
1034
1035 systems a size much greater than 20 μm and hence suitable for nasal delivery [49]. This
1036
1037 dimensional evaluation was confirmed by laser diffraction analysis which gave a volume
1038
1039 median diameter of $68.5 \pm 3.1 \mu\text{m}$, $76.3 \pm 5.2 \mu\text{m}$ and $84.5 \pm 8.1 \mu\text{m}$ for LM-Res, LM-Res-Ch
1040
1041 and LM-Res-Ch-plus, respectively. Zeta potential measurements indicated a negative value
1042
1043 ($-12.7 \pm 2.1 \text{ mV}$) for the uncoated particles whereas the chitosan-coated LM-Res-Ch and LM-
1044
1045 Res-Ch-plus exhibited positive zeta potential values which increased with the increase of the
1046
1047 chitosan concentration used for their preparation, respectively 24.0 ± 4.7 and $44.6 \pm 3.1 \text{ mV}$.
1048
1049 The change of the surface charge from a negative value to a positive values following coating
1050
1051 of the lipid particles demonstrated the efficient adsorption of the cationic biopolymer on the
1052
1053 particle surface. Moreover, the marked increase in the absolute zeta potential value for the
1054
1055 coated particles should ensure a higher stability for these systems.
1056
1057
1058
1059
1060
1061
1062

3.2. Permeation studies

The cells of the olfactory epithelium in the nasal cavity are tightly connected by “tight junctions”, constituted by a series of membrane proteins interacting with components of the cytoskeleton [48]. In order to evaluate the potential influence of the LMs without or with chitosan coating on the permeability properties of resveratrol, we have performed *in vitro* permeation experiments across monolayers of cells strictly connected by tight junctions. Unfortunately, the RPMI 2650 cell line, derived from a human nasal anaplastic squamous cell carcinoma of the nasal septum, was unsuitable for the evaluation of nasal transport, being unable to form a tight cell layer, a phenomenon caused by poor differentiation and lack of polarization of cells [50,51].

As a consequence, for permeation studies, the normal human colon mucosal epithelial cell line NCM460 [52] was chosen as an *in vitro* epithelial model, being this type of cells able to create monolayers tightly connected, as evidenced by TEER values of about 160 $\Omega\cdot\text{cm}^2$. Similar studies have been previously performed with Caco-2 cells [53], however in the present investigation the established NCM460 line was selected because in Caco-2 cell line changes in growth characteristics (monolayers/multilayers) are known to occur due to the loss of contact inhibition and polarization in transformed cell [54,55]. Moreover, as NCM460 cells are not of tumor origin, they retain the physiological characteristics of the human epithelia more closely compared to the pathologically transformed cell lines [55,56]. In order to simulate a nasal administration, the powders of raw resveratrol and the microparticulate systems were introduced in the apical compartments of the “Millicell” systems at levels which achieve the drug saturation. The permeation profiles of raw resveratrol across the Millicell filters alone or coated by monolayers obtained by NCM460 cells are reported in Figure 3,

1122 where the cumulative concentrations in the receiving compartments are shown. Figure 3
1123 reports also the permeation profiles of both raw resveratrol in the presence of unloaded
1124 microparticles and the drug encapsulated in the different microparticulate systems. The
1125 profiles are referred to the transport from the apical to basolateral compartments. The
1126 cumulative amounts in the receiving compartments showed a linear profile within 40 min in
1127 all cases ($R \geq 0.976$, $P \leq 0.02$) indicating constant permeation conditions within this time
1128 range. The apparent permeability coefficients (P_{app}) of resveratrol (Table 1) have been
1129 calculated according to eq. (1), on the basis of the resulting slopes of the linear fits and the
1130 resveratrol concentrations detected in the apical compartments after 40 min of incubation of
1131 the powders (Table 1), chosen as the approximate apical concentrations. A comparison of the
1132 P_{app} values of free resveratrol obtained in the presence ($518 \pm 8 \times 10^{-4}$ cm/min) and in the
1133 absence ($820 \pm 89 \times 10^{-4}$ cm/min) of NCM460 cell monolayers indicated a significantly
1134 lower permeation of the drug in the presence of cells ($P < 0.001$), confirming the validity of
1135 the monolayer as an *in vitro* model of a physiologic barrier. This behavior appeared in
1136 agreement with the transepithelial electrical resistance (TEER) values (about $160 \Omega \cdot \text{cm}^2$)
1137 attributed to the monolayers before their incubation with the powders (Table 1). The presence
1138 of the unloaded LMs induced a significant decrease of the resveratrol P_{app} value ($326 \pm 7 \times$
1139 10^{-4} cm/min) across the monolayer ($P < 0.05$), whereas this phenomenon was not observed
1140 with the unloaded microparticles LMs-Ch, coated with chitosan ($P_{app} = 480 \pm 36 \times 10^{-4}$
1141 cm/min). Interestingly, the unloaded microparticles LMs-Ch-plus, obtained in the presence of
1142 a chitosan solution of higher concentration, induced a significant increase ($P < 0.05$) of the
1143 resveratrol P_{app} value ($678 \pm 78 \times 10^{-4}$ cm/min). This effect can be attributed to the well-
1144 known ability of chitosan to reversibly open the tight junctions between cells [56,57], as
1145 demonstrated by the drastic decrease ($P < 0.001$) of the TEER value of the NCM460
1146 monolayer observed during the incubation of resveratrol with LMs-Ch-plus (TEER decreased
1147
1148
1149
1150
1151
1152
1153
1154
1155
1156
1157
1158
1159
1160
1161
1162
1163
1164
1165
1166
1167
1168
1169
1170
1171
1172
1173
1174
1175
1176
1177
1178
1179
1180

1181
1182
1183 from 150 ± 8 to $41 \pm 3 \Omega \cdot \text{cm}^2$, Table 1). It is important to remark that the incubation of
1184
1185 resveratrol alone, or in the presence of LMs or LMs-Ch unloaded microparticles, did not
1186
1187 induce any significant effect on TEER values of the NCM460 monolayer (Table 1). Similarly,
1188
1189 the loaded microparticles LMs-Res and LMs-Res-Ch did not influence the TEER values of
1190
1191 the monolayer (Table 1), whereas a significant decrease ($P < 0.001$) was observed during
1192
1193 incubation of the loaded microparticles, LMs -Res-Ch-plus (TEER decreased from 150 ± 7 to
1194
1195 $103 \pm 5 \Omega \cdot \text{cm}^2$, Table 1). Among the loaded microparticles, only those (LMs-Res-Ch-plus)
1196
1197 which produced a decrease of the NCM460 monolayer TEER value, significantly increase (P
1198
1199 < 0.001) the resveratrol P_{app} up to $750 \pm 98 \times 10^{-4} \text{ cm/min}$ (Table1). Therefore, this
1200
1201 microparticulate system represents a promising strategy for the enhancement of the resveratrol
1202
1203 uptake in the central nervous system, following its nasal administration.
1204
1205
1206
1207
1208

1209 3.3. *In vivo resveratrol administration*

1210
1211 Taking into account that the resveratrol loaded microparticles based on stearic acid (LMs-
1212
1213 Res) were characterized by a satisfactory encapsulation efficiency and release properties and
1214
1215 that the chitosan-coated LMs-Res-Ch-plus were able to promote the resveratrol permeation
1216
1217 across cell monolayers, these microparticulate systems (i.e., LMs-Res and LMs-Res-Ch-plus)
1218
1219 were tested for *in vivo* nasal administration of resveratrol in rats, in order to examine the
1220
1221 potential uptake of the polyphenol in the CNS. In particular, the nasal administration of
1222
1223 resveratrol was performed using the following different formulations: (i) a suspension of raw
1224
1225 resveratrol powder in water, chosen as control, (ii) a suspension of raw resveratrol powder in
1226
1227 a chitosan hydrochloride solution, (iii) a suspension of LMs-Res microparticles in water and
1228
1229 (iv) a suspension of LMs-Res-Ch-plus microparticles in water. The results were compared
1230
1231 with those obtained after the intravenous infusion of resveratrol into the rats.
1232
1233
1234
1235
1236
1237
1238
1239

3.4. Intravenous administration of resveratrol

For the assay of resveratrol in rat blood, conventional liquid extraction followed by centrifugation and solvent removal was initially used as sample preparation method [58]. However, with this pre-treatment procedure, a peak interfering with the determination of resveratrol was observed in the UV chromatogram of the blood sample. Moreover, unsatisfactory recoveries (< 10%) were obtained for resveratrol. In order to overcome this drawback, purification methods based on solid-phase extraction techniques were examined. Disposable C18-bonded silica cartridge were selected since they provide the broadest applicability for pre-treatment of biological fluids. Several C18 silica cartridges (Isolute C18, Isolute MF C18 and Bond-Elut C18) were evaluated using rat blood spiked with resveratrol and the internal standard (quercetin). The highest resveratrol recovery rate (> 80.3%) was achieved by the non-encapped C18-bonded silica sorbent (Isolute MF C18), probably due to enhance analyte retention through the additional interaction associated with the very accessible silanol groups and therefore this cartridge was selected for the extraction of resveratrol from blood specimens. The analysis of rat blood samples following the intravenous infusion of 0.2 mg of resveratrol indicated that the drug concentration in the blood stream decreased over time from a value of about 7.5 µg/mL (Fig. 4) with an apparent first order kinetic, as confirmed by the linearity of the semilogarithmic plot reported in the inset of Figure 4 (n = 4, R = 0.980, P < 0.0001), and a half-life of 129 ± 8 min. This value is comparable with that observed in humans following resveratrol administration [59]. No resveratrol was detected in CSF of rats within 180 min after the end of intravenous infusion of the drug.

3.5. Nasal administration of resveratrol

Following nasal administration of pure resveratrol (0.2 mg) as a water suspension, no detectable amounts of the drug in the rat blood or CSF were observed within 180 min of administration. In contrast, the nasal administration of the same dose of resveratrol suspended in the chitosan hydrochloride solution (7.5 mg/mL), produced detectable amounts of the drug in the CSF of the rats, as reported in Figure 5. In particular, the resveratrol C_{\max} was obtained 60 min after nasal administration of the suspension with a value of $1.30 \pm 0.30 \mu\text{g/mL}$.

The nasal administration of the same amount of resveratrol encapsulated in LMs-Res microparticles produced an effect similar to that achieved by the suspension of resveratrol in chitosan solution: indeed, the resveratrol C_{\max} in CSF was obtained 60 min after nasal administration of the LMs-Res suspension with a value of $0.79 \pm 0.15 \mu\text{g/mL}$. Moreover, in this case resveratrol was also detected at 30 and 120 min though at lower concentrations, respectively $0.020 \pm 0.05 \mu\text{g/mL}$ and $0.15 \pm 0.03 \mu\text{g/mL}$ (Figure 5).

A drastic increase of the polyphenol uptake in the CSF of the rats was obtained by administration of the water suspension of the chitosan-coated LMs-Res-Ch-plus microparticles containing an equivalent amount of resveratrol (0.2 mg). In this case the drug C_{\max} in CSF, observed 60 min after nasal administration, reached a value of $9.7 \pm 1.9 \mu\text{g/mL}$ (Figure 5), which was an order of magnitude higher than that obtained after the nasal administration of the uncoated LMs-Res microparticles. Finally, no resveratrol was detected in the bloodstream of rats within 180 min after nasal administration of the suspensions of resveratrol in chitosan hydrochloride solution, LMs-Res or LMs-Res-Ch-plus microparticles in water.

The areas under the concentration (AUC) curve values (mean \pm SD) obtained for resveratrol in the rat CSF after the nasal administration of the drug suspension in the chitosan hydrochloride solution, the LMs-Res and the LMs-Res-Ch-plus microparticles were 54 ± 13 ,

1358
1359
1360 45 ± 5 and $554 \pm 67 \mu\text{g}\cdot\text{mL}\cdot\text{min}^{-1}$, respectively (Figure 6). The ratio between the AUC values
1361
1362 of LMs-Res-Ch-plus and those of resveratrol or LMs-Res formulations were 10.2 or 12.3,
1363
1364 respectively, indicating the superior ability of the chitosan coated microparticles to induce the
1365
1366 resveratrol uptake in CSF of rats after nasal administration, with respect to the other two
1367
1368 formulations tested ($P < 0.001$).

1371 The markedly higher levels of resveratrol reaching the brain attained by the LMs-Res-Ch-
1372
1373 plus formulation can be ascribed to enhance polyphenol absorption through the mucosal tissue
1374
1375 due to chitosan induced reversible opening of the tight junctions in the cell membranes of the
1376
1377 nasal epithelium [56], as also suggested by the *in vitro* permeation studies on the NCM460
1378
1379 cell line. The observed C_{max} values at 60 min (Figure 5) suggests that resveratrol can reach the
1380
1381 CNS by paracellular diffusion across the olfactory mucosa, rather than by the transneuronal
1382
1383 pathway which is known to require at least 24 hours [60]. In addition, the mucoadhesive
1384
1385 nature of the chitosan-coated microparticles should delay the mucociliary clearance
1386
1387 prolonging the retention of the formulation on the nasal cavity. The obtained data indicate
1388
1389 that the concentration of the chitosan coating of the LMs is critical for efficient brain targeting
1390
1391 of resveratrol following nasal administration, since the marked enhancement in CSF
1392
1393 bioavailability was achieved only the LMs-Res-Ch-plus system, coated with the chitosan
1394
1395 solution at higher concentration (8.75%, w/v). Moreover, the amount of resveratrol measured
1396
1397 in the rat brain following administration of the LMs-Res-Ch-plus formulation is comparable
1398
1399 and higher than the level which has been shown to elicit *in vivo* neuroprotective activity [19].
1400
1401 Nasal resveratrol formulations based on nanoemulsions and nanosuspensions have been
1402
1403 recently described by other authors [18,19,61]. Although a significant increase (about 3-7 fold
1404
1405 increase) in the polyphenol brain bioavailability was achieved compared to conventional
1406
1407 administrations, a partial distribution (about 24-35%) of the polyphenol in the systemic
1408
1409 circulation was observed [18,19,61]. Conversely, the LM system developed here attained
1410
1411
1412
1413
1414
1415
1416

1417
1418
1419 complete targeting of resveratrol to the brain, being resveratrol undetectable in the
1420
1421 bloodstream of rats after the nasal administration of the chitosan-coated resveratrol-loaded
1422
1423 lipid microparticles (LMs-Res-Ch-plus). The high selectivity achieved by microparticle
1424
1425 system developed in this study, should reduce the amount of drug required for the expected
1426
1427 pharmacological effect.
1428

1429 1430 1431 1432 **4. Conclusions**

1433
1434 Resveratrol-loaded LMs uncoated and coated with chitosan were developed in this study
1435
1436 and evaluated *in vitro* and *in vivo* as a carrier system to enhance the targeting of resveratrol to
1437
1438 the brain via nasal administration. To the best of our knowledge, the effect of microparticulate
1439
1440 powder carrier on the *in vivo* nose to brain uptake of resveratrol has not been reported before.
1441
1442 Advantages of the LMs system described here include biodegradability of their components,
1443
1444 specific brain delivery, ease of administration as well as non-invasiveness. Pharmacokinetic
1445
1446 studies indicated that the intranasal administration of the LMs-Res-Ch-plus particles
1447
1448 produced a marked increase in the bioavailability of resveratrol in the brain which should
1449
1450 enhance its neuroprotective effect for the treatment of neurological disorders.
1451
1452

1453 1454 1455 **Acknowledgements**

1456
1457 This study was supported by a grant from the University of Ferrara (F.A.R. 2015) and the
1458
1459 “Contributo 5 per mille, anno 2014, Università di Ferrara ”.
1460
1461

1462 1463 1464 **Declaration of interest**

1465
1466 The authors declare no conflicts of interest.
1467
1468
1469
1470
1471
1472
1473
1474
1475

1476
1477
1478
1479
1480
REFERENCES
1481

- 1482 [1] U. Stervbo, O. Vang, C. Bonnesen, A review of the content of the putative
1483 chemopreventive phytoalexin resveratrol in red wine, *Food Chem.* 101(2007) 449-
1484 457.
1485
1486
1487
1488 [2] A. Amri, J.C. Chaumeil, S. Sfar, C. Charrueau, Administration of resveratrol: what
1489 formulation solutions to bioavailability limitations?, *J. Control. Release* 158 (2012)
1490 182-193.
1491
1492
1493
1494 [3] D. Bonnefont-Rousselot, Resveratrol and Cardiovascular Diseases, *Nutrients* 8 (2016)
1495 E 250.
1496
1497
1498 [4] N.G.A. Vallianou, A. Evangelopoulos, C. Kazazis, Resveratrol and diabetes, *Rev.*
1499 *Diabet Stud.*10 (2013) 236-242.
1500
1501
1502 [5] M. Venigalla, S. Sonogo, E. Gyengesi, M. J.Sharman, G. Münch, Novel promising
1503 therapeutics against chronic neuroinflammation and neurodegeneration in Alzheimer's
1504 disease, *Neurochem. Int.* 95 (2016) 63-74.
1505
1506
1507 [6] N. Zang, S. Li, W. Li, X. Xie, L. Ren, X. Long, X. Jun, D. Yu, F. Zhou, X.
1508 Fadi, L. Enmei, Resveratrol suppresses persistent airway inflammation and
1509 hyperresponsiveness might partially via nerve growth factor in respiratory syncytial
1510 virus-infected mice, *Int. Immunopharmacol.* 28 (2015) 121-128.
1511
1512
1513 [7] N.G. Vallianou, A. Evangelopoulos, E. Geladari, C. Kazazis, Resveratrol and Cancer,
1514 *Hospital Chronicles* 10 (2015) 137-144.
1515
1516
1517 [8] S. Das, D.K. Das, Anti-inflammatory responses of resveratrol, *Inflammation &*
1518 *Allergy-Drug Targets (Formerly Current Drug Targets-Inflammation & Allergy)*, 6
1519 (2007) 168-173.
1520
1521
1522
1523
1524
1525
1526
1527
1528
1529
1530
1531
1532
1533
1534

- 1535
1536
1537
1538
1539
1540
1541
1542
1543
1544
1545
1546
1547
1548
1549
1550
1551
1552
1553
1554
1555
1556
1557
1558
1559
1560
1561
1562
1563
1564
1565
1566
1567
1568
1569
1570
1571
1572
1573
1574
1575
1576
1577
1578
1579
1580
1581
1582
1583
1584
1585
1586
1587
1588
1589
1590
1591
1592
1593
- [9] J. H. Yoon, S.J. Baek, Molecular targets of dietary polyphenols with anti-inflammatory properties, *Yonsei Med. J.* 46 (2005) 585-596.
- [10] S.S. Leonard, C. Xia, B. H. Jiang, B. Stinefelt, H. Klandorf, G. K. Harris, X. Shi, Resveratrol scavenges reactive oxygen species and effects radical-induced cellular responses, *Biochem. Bioph. Res. Co.* 309 (2003) 1017-1026.
- [11] D. W. Anderson, K. A. Bradbury, J. S. Schneider, Neuroprotection in Parkinson models varies with toxin administration protocol. *Eur. J. Neurosci.* 24 (2006) 3174-3182.
- [12] D. Albani, L. Polito, A. Signorini, G. Forloni, Neuroprotective properties of resveratrol in different neurodegenerative disorders, *Biofactors* 36 (2010) 370-376.
- [13] P. Ganesan, H. M. Ko, I. S. Kim, D.K. Choi, Recent trends in the development of nanophytobioactive compounds and delivery systems for their possible role in reducing oxidative stress in Parkinson's disease models, *Int. J. Nanomed.* 10 (2015) 6757-6772.
- [14] A. R. Neves, J. F. Queiroz, S. Reis, Brain-targeted delivery of resveratrol using solid lipid nanoparticles functionalized with apolipoprotein E, *J. Nanobiotechnol.* 14 (2016) 27-37.
- [15] M. D. Pandareesh, R. B. Mythri, M. S. Bharath, Bioavailability of dietary polyphenols: Factors contributing to their clinical application in CNS diseases, *Neurochem. Int.* 89 (2015) 198-208.
- [16] M. Mokni, S. Elkahoui, F. Limam, M. Amri, E. Aouani, Effect of resveratrol on antioxidant enzyme activities in the brain of healthy rat, *Neurochem. Res.* 32 (2007) 981-987.
- [17] K.A. Potter, A.C. Buck, W.K. Self, M.E. Callanan, S. Sunil, J.R. Capadona, The effect of resveratrol on neurodegeneration and blood brain barrier stability surrounding

- 1594
1595
1596 intracortical microelectrodes, *Biomaterials* 34 (2013) 7001–7015.
1597
- [18] J. Hao, J. Zhao, S. Zhang, T. Tong, Q. Zhuang, K. Jin, W. Chen, H. Tang, Fabrication
1598 of an ionic-sensitive in situ gel loaded with resveratrol nanosuspensions intended for
1599 direct nose-to-brain delivery, *Colloids Surf.B:Biointerfaces* 147 (2016) 376-386.
1600
1601
1602
1603
1604
- [19] M. Nasr, Development of an optimized hyaluronic acid-based lipidic nanoemulsion
1605 co-encapsulating two polphenols for nose to brain delivery, *Drug Deliv.* 23 (2016)
1606 1444-1452.
1607
1608
1609
1610
- [20] D. Delmas, V. Aires, E. Limagne, P. Dutartre, F. Mazué, F. Ghiringhelli, N. Latruffe,
1611 Transport, stability, and biological activity of resveratrol, *Annals of the New York*
1612 *Academy of Sciences* 1215 (2011) 48-59.
1613
1614
1615
1616
- [21] A.R. Neves, M. Lúcio, J.L.C. Lima, S. Reis, Resveratrol in medicinal chemistry: a
1617 critical review of its pharmacokinetics, drug-delivery, and membrane interactions,
1618 *Curr. Med. Chem.* 19 (2012) 1663-1681.
1619
1620
1621
1622
1623
- [22] S. Scalia, V. Trotta, V. Iannuccelli, A. Bianchi, Enhancement of in vivo human skin
1624 penetration of resveratrol by chitosan-coated lipid microparticles. *Colloids Surf B :*
1625 *Biointerfaces*, 135 (2015) 42-49.
1626
1627
1628
1629
- [23] I. Martignoni, V. Trotta, W.-H. Lee, C.-Y. Loo, M. Pozzoli, P.M. Young, S. Scalia, D.
1630 Traini, Resveratrol solid lipid microparticles as dry powder formulation for nasal
1631 delivery, characterization and in vitro deposition study, *J. Microencapsul.* 33 (2016)
1632 735-742.
1633
1634
1635
1636
1637
1638
- [24] S. Scalia, P.M. Young, D. Traini, Solid lipid microparticles as an approach to drug
1639 delivery, *Expert Opin. Drug Del.* 12 (2015) 583-599.
1640
1641
1642
- [25] S. Jaspert, G. Piel, L. Delattre, B. Evrard, Solid lipid microparticles: formulation,
1643 preparation, characterisation, drug release and applications, *Expert Opin. Drug Del.* 2
1644 (2005) 75-87.
1645
1646
1647
1648
1649
1650
1651
1652

- 1653
1654
1655 [26] R. Watkins, L. Wu, C. Zhang, R.M. Davis, B. Xu, Natural product-based
1656
1657 nanomedicine: recent advances and issues, *Int. J. Nanomed.* 10 (2015) 6055-6074.
1658
1659 [27] Q. Wang, J. Xu, G.E. Rottinghaus, A. Simonyi, D. Lubahn, G.Y. Sunb, A.Y. Suna,
1660
1661 Resveratrol protects against global cerebral ischemic injury in gerbils, *Brain Res.* 958
1662
1663 (2002) 439-447.
1664
1665 [28] R.S.Turner, R.G. Thomas, S. Craft, C.H.van Dyck, J. Mintzer., B.A.Reynolds, J.B.
1666
1667 Brewer, R.A. Rissman, R. Raman, P.S. Aisen, A randomized, double-blind, placebo-
1668
1669 controlled trial of resveratrol for Alzheimer disease, *Neurology* 85 (2015) 1383-1391.
1670
1671
1672 [29] J. M. Smoliga, O. Blanchard, Enhancing the Delivery of Resveratrol in Humans: If
1673
1674 Low Bioavailability is the Problem, What is the Solution?, *Molecules* 19 (2014)
1675
1676 17154-17172.
1677
1678 [30] T. B. Devkar, A. R. Tekade, K.R. Khandelwal, Surface engineered nanostructured
1679
1680 lipid carriers for efficient nose to brain delivery of ondansetron HCl using Delonix
1681
1682 regia gum as a natural mucoadhesive polymer, *Colloids Surf. B Biointerfaces* 122
1683
1684 (2014) 143-150.
1685
1686 [31] C. Rodriguez-Nogales, E. Garbayo, M.M. Carmona Abellàn, M.R. Luquin, Brain
1687
1688 aging and Parkinson's disease: new therapeutic approaches using drug delivery
1689
1690 systems, *Maturitas* 84 (2016) 25-31.
1691
1692 [32] S. Wohlfart, S. Gelperina, J. Kreuter, Transport of drugs across the blood–brain barrier
1693
1694 by nanoparticles, *J. Control. Release* 161 (2012) 264-273.
1695
1696 [33] J.J. Lochhead, R.G. Thorne, Intranasal delivery of biologics to the central nervous
1697
1698 system, *Adv. Drug Deliver. Rev.* 64 (2012) 614-628.
1699
1700 [34] J.M. Fine, A.C. Forsberg, D.B. Renner, K.A. Faltesek, K.G. Mohan, J.C. Wong, L.C.
1701
1702 Arneson, J.M. Crow, W.H. 2nd Frey, L.R. Hanson. Intranasally-administered
1703
1704
1705
1706
1707
1708
1709
1710
1711

- 1712
1713
1714 deferoxamine mitigates toxicity of 6-OHDA in a rat model of Parkinson's disease,
1715
1716 Brain Res. 1574 (2014) 96-104.
1717
- [35] J. Freiherr, M. Hallschmid, W.H. 2nd Frey, Y.F. Brünner, C.D. Chapman, C.
1718
1719 Hölscher, S. Craft, F.G. De Felice, C. Benedict. Intranasal insulin as a treatment for
1720
1721 Alzheimer's disease: a review of basic research and clinical evidence, CNS Drugs. 27
1722
1723 (2013) 505-514.
1724
1725
- [36] F. Buttini, P. Colombo, A. Rossi, F. Sonvico, G. Colombo, Particles and powders:
1726
1727 tools of innovation for non-invasive drug administration, J. Control. Release. 161
1728
1729 (2012) 693-702.
1730
1731
- [37] A.D. Sezer, E. Cevher, Topical drug delivery using chitosan nano-and microparticles,
1732
1733 Expert Opin. Drug Del. 9 (2012) 1129-1146.
1734
1735
- [38] K. Felgenhauer, Protein size and CSF composition, Klin. Wochenschr. 52 (1974)
1736
1737 1158–1164.
1738
1739
- [39] A. Madu, C. Cioffe, U. Mian, M. Burroughs, E. Tuomanen, M. Mayers, E. Schwartz,
1740
1741 M. Miller, Pharmacokinetics of fluconazole in cerebrospinal fluid and serum of
1742
1743 rabbits: validation of an animal model used to measure drug concentrations in
1744
1745 cerebrospinal fluid, Antimicrob, Agents Chemother. 38 (1994) 2111–2115.
1746
1747
1748
- [40] V. Ferretti, A. Dalpiaz, V. Bertolasi, L. Ferraro, S. Beggiato, F. Spizzo, E. Spisani, B.
1749
1750 Pavan, Indomethacin co-Crystals and their parent mixtures: Does the intestinal barrier
1751
1752 recognize them differently?, Mol. Pharmaceutics 12 (2015) 1501–1511.
1753
1754
1755
- [41] P. Artursson, J. Karlson, Correlation between oral absorption in humans and apparent
1756
1757 drug permeability coefficients in human intestinal epithelial (Caco-2) cells, Biochem.
1758
1759 Biophys. Res. Commun. 175 (1991) 880–885.
1760
1761
- [42] D. Pal, C. Udata, A. K. Mitra, Transport of cosalane, a highly lipophilic novel anti-
1762
1763 HIV agent, across Caco-2 cell monolayers, J. Pharm. Sci. 89 (2000) 826–833.
1764
1765
1766
1767
1768
1769
1770

- 1771
1772
1773
1774
1775
1776
1777
1778
1779
1780
1781
1782
1783
1784
1785
1786
1787
1788
1789
1790
1791
1792
1793
1794
1795
1796
1797
1798
1799
1800
1801
1802
1803
1804
1805
1806
1807
1808
1809
1810
1811
1812
1813
1814
1815
1816
1817
1818
1819
1820
1821
1822
1823
1824
1825
1826
1827
1828
1829
- [43] S. Raje, J. Cao, A. H. Newman, H. Gao, N. D. Eddington, Evaluation of the blood-brain barrier transport, population pharmacokinetics, and brain distribution of benzotropine analogs and cocaine using in vitro and in vivo techniques, *J. Pharmacol. Exp. Ther.* 307 (2003) 801–808.
- [44] M.P. Van den Berg, S.G. Romeijn, J.C. Verhoef, F.W. Merkus, Serial cerebrospinal fluid sampling in a rat model to study drug uptake from the nasal cavity, *J. Neurosci. Methods* 116 (2002) 99–107.
- [45] A. Dalpiaz, L. Ferraro, D. Perrone, E. Leo, V. Iannuccelli, B. Pavan, G. Paganetto, S. Beggiato, S. Scalia, Brain uptake of a zidovudine prodrug after nasal administration of solid lipid microparticles, *Mol. Pharmaceutics* 11 (2014) 1550–1561.
- [46] J. L. Meek, N. H. Neff, Is cerebrospinal fluid the major avenue for the removal of 5-hydroxyindoleacetic acid from the brain?, *Neuropharmacology* 12 (1973) 497–499.
- [47] H. Davson, K. Welch, M.B. Segal, The secretion of the cerebrospinal fluid, in: H. Davson, K. Welch, M.B. Segal (Eds.), *Physiology and Pathophysiology of the Cerebrospinal fluid*, Churchill Livingstone, London, 1987, pp. 189–246.
- [48] L. Casettari, L. Illum, Chitosan in nasal delivery systems for therapeutic drugs, *J. Control. Release* 190 (2014) 189-200.
- [49] P. Kippax, J. Suman, G. Williams, Understanding the requirements for effective nasal drug delivery, *Pharm. Technol. Europe* 9 (2010) 58-65.
- [50] A. De Fraissinette, R. Brun, H. Felix, J. Vonderscher, A. Rummelt, Evaluation of the human cell line RPMI 2650 as an in vitro nasal model, *Rhinology* 33 (1995) 194-198.
- [51] S. Dimova, M.E. Brewster, M. Noppe, M. Jorissen, P. Augustijns, The use of human nasal in vitro cell systems during drug discovery and development, *Toxicol. In Vitro* 19 (2005) 107-122.

- 1830
1831
1832
1833 [52] M.P. Moyer, L. Manzano, R. Merriman, J. Stauffer, L.R. Tanzer, NCM460, a normal
1834 human colon mucosal epithelial cell line, *In Vitro Cell. Dev. Biol. Anim.* 32 (1996)
1835 315–317.
1836
1837
1838
1839 [53] G. Rassa, E. Soddu, M. Cossu, A. Brundu, G. Cerri, N. Marchetti, L. Ferraro, R.F.
1840 Regan, P. Giunchedi, E. Gavini, A. Dalpiaz, Solid microparticles based on chitosan or
1841 methyl- β cyclodextrin: a first formulative approach to increase the nose-to-brain
1842 transport of deferoxamine mesylate, *J. Control. Release* 201 (2015) 68-77.
1843
1844
1845
1846
1847 [54] B. Rothen-Rutishauser, A. Braun, M. Gunthert, H. Wunderli-Allenspach, Formation of
1848 multilayers in the caco-2 cell culture model: a confocal laser scanning microscopy
1849 study, *Pharm. Res.* 17 (2000) 460–465.
1850
1851
1852
1853 [55] P. Marchetti, B. Pavan, D. Simoni, R. Baruchello, R. Rondanin, C. Mischianti, G.
1854 Feriotto, L. Ferraro, R.M. Hsu, L.C. Lee, A. Dalpiaz, A novel hybrid drug between
1855 two potent anti-tubulin agents as a potential prolonged anticancer approach, *Eur. J.*
1856 *Pharm. Sci.* 91 (2016) 50-63.
1857
1858
1859
1860
1861 [56] L. Illum, Nasal drug delivery – possibilities, problems and solutions, *J. Control.*
1862 *Release* 87 (2003) 187–198.
1863
1864
1865
1866 [57] B. Pavan, G. Paganetto, D. Rossi, A. Dalpiaz, Multidrug resistance in cancer or
1867 inefficacy of neuroactive agents: innovative strategies to inhibit or circumvent the
1868 active efflux transporters selectively, *Drug Discovery Today* 19 (2014) 1563-1571.
1869
1870
1871
1872 [58] P. Ramalingam, Y.T.Ko , Validated LC-MS/MS method for simultaneous
1873 quantification of resveratrol levels in mouse plasma and brain and its application to
1874 pharmacokinetic and brain distribution studies, *J. Pharm. Biomed. Anal.* 119 (2016)
1875 71-75
1876
1877
1878
1879
1880 [59] L. Almeida, M. Vaz-da-Silva, A. Falcão, E. Soares, R. Costa, A.I. Loureiro, C.
1881 Fernandes-Lopes, J.F. Rocha, T. Nunes, L. Wright, P. Soares-da-Silva,
1882
1883
1884
1885
1886
1887
1888

1889
1890
1891 Pharmacokinetic and safety profile of transresveratrol in a rising multiple-dose study
1892 in healthy volunteers, *Mol. Nutr. Food Res.* 53 (2009) S7-S15.
1893

1894
1895 [60] Illum, L. Transport of drugs from the nasal cavity to the central nervous system. *Eur.*
1896 *J. Pharm. Sci.* 11 (2000) 11, 1-18.
1897

1898
1899 [61] R. Pangeni, S. Sharma, G. Mustafa, J. Ali, S. Baboota, Vitamin E loaded resveratrol
1900 nanoemulsion for brain targeting for the treatment of Parkinson's disease by reducing
1901 oxidative stress, *Nanotechnology* 25 (2014) E485102.
1902
1903
1904
1905
1906
1907
1908
1909
1910
1911
1912
1913
1914
1915
1916
1917
1918
1919
1920
1921
1922
1923
1924
1925
1926
1927
1928
1929
1930
1931
1932
1933
1934
1935
1936
1937
1938
1939
1940
1941
1942
1943
1944
1945
1946
1947

Caption of Figures

Figure 1. Resveratrol dissolution and release profiles from LMs. Values are means \pm SD (n=5).

Figure 2. SEM micrographs of (A)LMs-Res, (B) LMs-Res-Ch and (C) LMs-Res-Ch plus

Figure 3. Permeation kinetics of resveratrol after introduction in the “Millicell” apical compartments of powders composed by resveratrol in the absence (Res) or in the presence of unloaded microparticles (LMs, LMs-Ch, LMs-Ch-plus) and by the loaded microparticles (LMs-Res, LMs-Res-Ch, LMs-Res-Ch-plus). The permeations were analyzed across monolayers obtained by NCM460 cells. The permeation of free resveratrol was analyzed across the Millicell filters alone (filter) or coated by monolayers (cells). The cumulative amounts in the basolateral receiving compartments were linear within 60 min ($R \geq 0.976$, $P \leq 0.02$). The resulting slopes of the linear fits were used for the calculation of permeability coefficients (P_{app}). All data are reported as mean \pm SD of four independent experiments.

Figure 4. Elimination profile of resveratrol after 0.20 mg infusion to rats. The elimination followed an apparent first order kinetic 60 min after the end of infusion, confirmed by the semilogarithmic plot reported in the inset (n = 4, r = 0.980, P < 0.0001). The half-life of resveratrol was calculated to be 129 ± 8 min. All data reported in the figure are expressed as the mean \pm SD of four independent experiments.

Figure 5. Resveratrol (Res) concentrations ($\mu\text{g/mL}$) detected in the CSF after the nasal administration of suspensions of powders constituted by the mixture of the drug and chitosan

2007
2008
2009 HCl and the loaded microparticles (LMs-Res and LMs-Res-Ch-plus). Each dose contained
2010
2011 200 µg of resveratrol. The data are expressed as the mean ± SD of four independent
2012
2013
2014 experiments.
2015
2016
2017

2018 **Figure 6.** Comparison of the AUC values obtained in the CSF of rats after the
2019
2020 nasal administration of 200 µg of resveratrol (Res) using different suspension of powders
2021
2022 constituted by the mixture of drug with chitosan and the loaded microparticles (LMs-Res and
2023
2024 LMs-Res-Ch-plus). The data are expressed as the mean ± SD of four independent
2025
2026 experiments. (*P < 0.001 *versus* Res + Chitosan HCl or *versus* LMs-Res)
2027
2028
2029
2030
2031
2032
2033
2034
2035
2036
2037
2038
2039
2040
2041
2042
2043
2044
2045
2046
2047
2048
2049
2050
2051
2052
2053
2054
2055
2056
2057
2058
2059
2060
2061
2062
2063
2064
2065

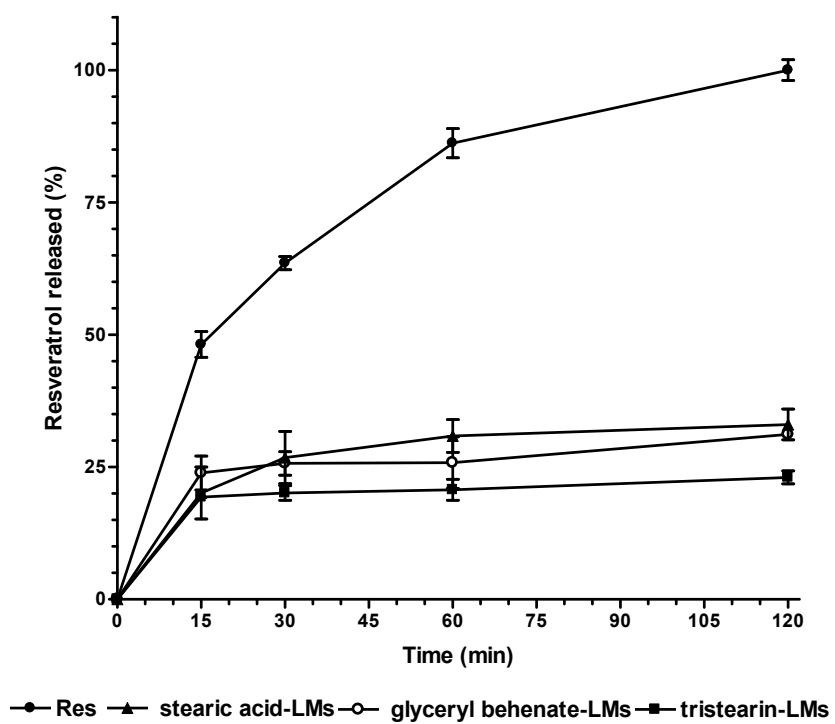


Figure 1

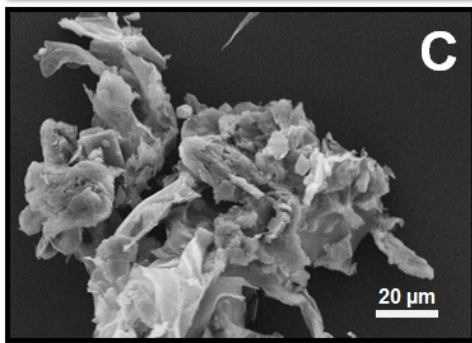
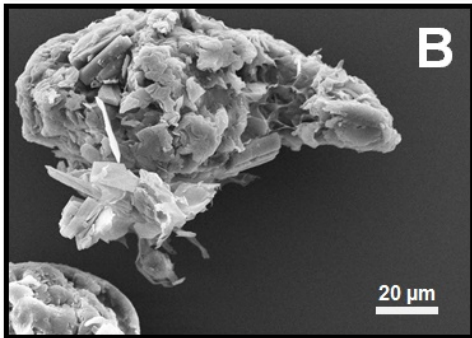
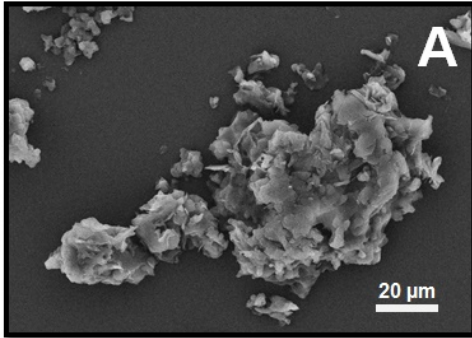


Figure 2

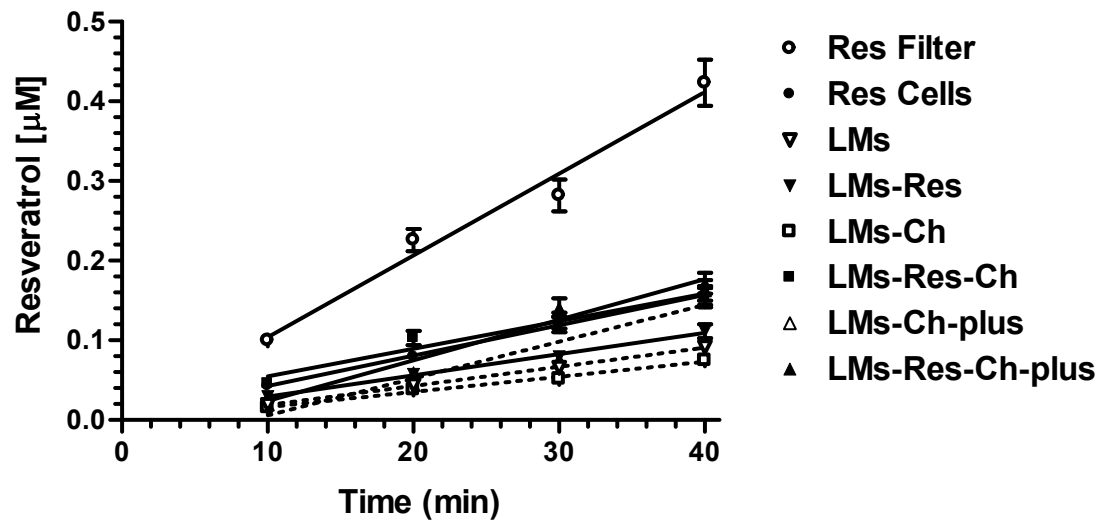


Figure 3

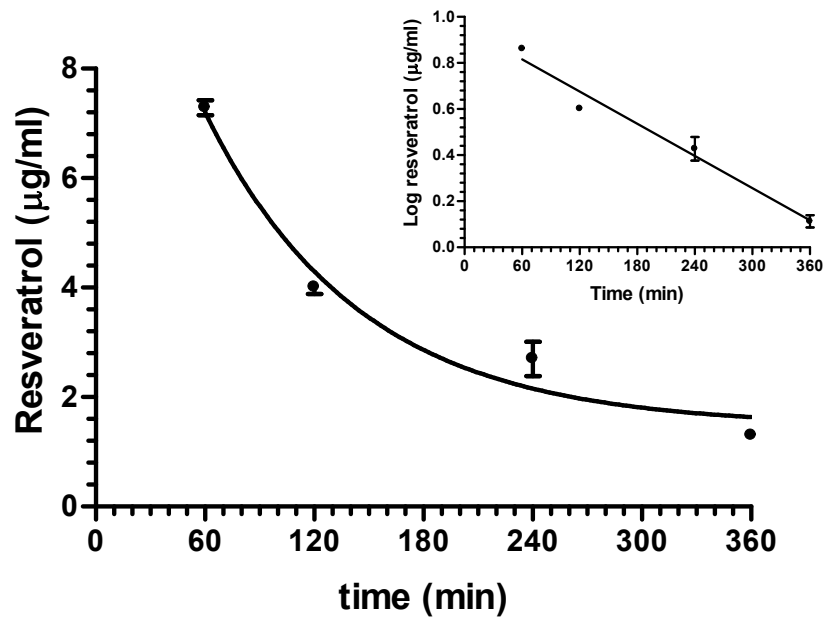


Figure 4

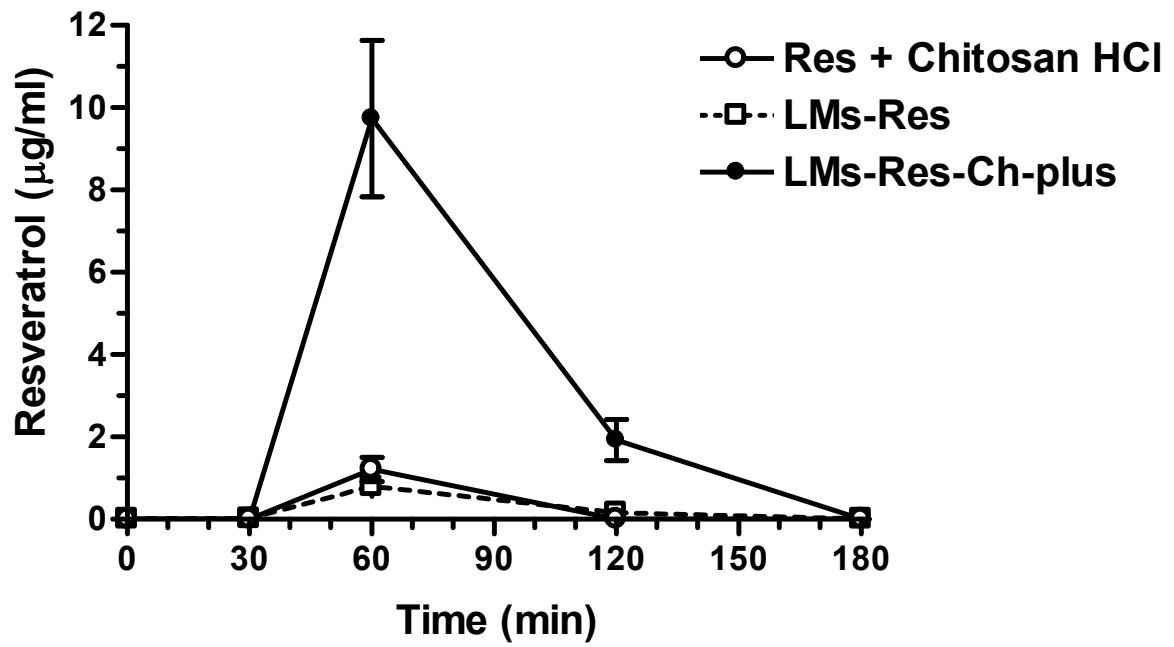


Figure 5

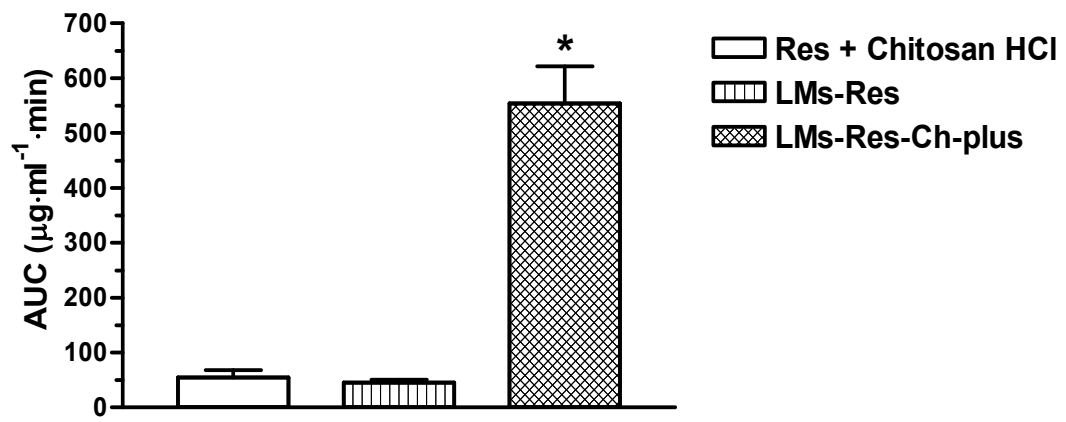


Figure 6

Table 1. Resveratrol permeation data obtained on “Millicell” filters alone (filter) or coated by NCM460 cell monolayers (cells). Resveratrol was introduced in the donor compartment both as raw powder, in the presence of unloaded microparticles or encapsulated in the microparticles. The resveratrol apical concentrations detected at the end of incubation (40 min) were employed for the calculation of the apparent permeation coefficients (P_{app}). The transepithelial electrical resistance (TEER) values were measured before (0 min) and at the end of incubation (40 min). All data related to permeation studies are reported as the mean \pm SD of four independent experiments.

Powder	Permeation condition	apical conc. at 40 min (μ M)	P_{app} ($\times 10^{-4}$ cm/min)	TEER ($\Omega \cdot \text{cm}^2$)	
				0 min	40 min
Resveratrol	cells	0.134 \pm 0,008	518 \pm 8	150 \pm 7	152 \pm 8
Resveratrol+LMs	cells	0.133 \pm 0.007	326 \pm 7*	159 \pm 8	166 \pm 9
LMs-Res	cells	0.125 \pm 0.007	390 \pm 20	161 \pm 9	148 \pm 7
Resveratrol+LMs-Ch	cells	0.074 \pm 0.004	480 \pm 36	150 \pm 8	152 \pm 8
LMs-Res-Ch	cells	0.128 \pm 0.008	510 \pm 80	152 \pm 9	148 \pm 8
Resveratrol+LMs-Ch-plus	cells	0.126 \pm 0.007	678 \pm 78*	150 \pm 8	41 \pm 3***
LMs-Res-Ch-plus	cells	0.121 \pm 0.007	750 \pm 98**	150 \pm 7	103 \pm 5***
Resveratrol	filter	0.219 \pm 0.011	820 \pm 89**	--	--

* $P < 0.05$ versus Resveratrol (cells) P_{app} value; ** $P < 0.001$ versus Resveratrol (cells) P_{app} value;

*** $P < 0.001$ versus TEER at “time 0” (0 min).